THE JOURNAL OF BIOLOGICAL CHEMISTRY
Vol. 280, No. 12, Issue of March 25, pp. 11648–11655, 2005
Printed in U.S.A.
© 2005 by The American Society for Biochemistry and Molecular Biology, Inc.

Oxidative Modifications and Aggregation of Cu,Zn-Superoxide Dismutase Associated with Alzheimer and Parkinson Diseases*

Received for publication, December 20, 2004, and in revised form, January 18, 2005
Published, JBC Papers in Press, January 19, 2005, DOI 10.1074/jbc.M414327200

Joungil Choi‡, Howard D. Rees‡§, Susan T. Weintraub¶, Allan I. Levey‡§, Lih-Shen Chin‡, and Lian Li‡‖

From the Departments of ‡Pharmacology and §Neurology, Center for Neurodegenerative Disease, Emory University School of Medicine, Atlanta, Georgia 30322-3090 and ¶Department of Biochemistry, University of Texas Health Science Center, San Antonio, Texas 78229

Although oxidative stress has been strongly implicated in the pathogenesis of Alzheimer disease (AD) and Parkinson disease (PD), the identities of specific protein targets of oxidative damage remain largely unknown. Here, we report that Cu,Zn-superoxide dismutase (SOD1), a key antioxidant enzyme whose mutations have been linked to autosomal dominant neurodegenerative disorder familial amyotrophic lateral sclerosis (ALS), is a major target of oxidative damage in AD and PD brains. By using a combination of two-dimensional gel electrophoresis, immunoblot analysis, and mass spectrometry, we have identified four human brain SOD1 isoforms with pI values of 6.3, 6.0, 5.7, and 5.0, respectively. Of these, the SOD1 pI 6.0 isoform is oxidatively modified by carbonylation, and the pI 5.0 isoform is selectively accumulated in AD and PD. Moreover, Cys-146, a cysteine residue of SOD1 that is mutated in familial ALS, is oxidized to cysteic acid in AD and PD brains. Quantitative Western blot analyses demonstrate that the total level of SOD1 isoforms is significantly increased in both AD and PD. Furthermore, immunohistochemical and double fluorescence labeling studies reveal that SOD1 forms proteinaceous aggregates that are associated with amyloid senile plaques and neurofibrillary tangles in AD brains. These findings implicate, for the first time, the involvement of oxidative damage to SOD1 in the pathogenesis of sporadic AD and PD. This work suggests that AD, PD, and ALS may share a common or overlapping pathogenic mechanism(s) that could potentially be targeted by similar therapeutic strategies.

Alzheimer disease (AD),[1] Parkinson disease (PD), and amyotrophic lateral sclerosis (ALS; also known as Lou Gehrig disease) are chronic neurodegenerative disorders characterized by selective neuronal death and the accumulation of insoluble proteinaceous deposits, such as senile plaques and neurofibrillary tangles in AD, Lewy bodies in PD, and hyaline- and skein-like inclusion bodies in ALS (1, 2). Increasing evidence indicates that oxidative stress plays a critical role in the pathogenesis of these slowly progressive neurodegenerative diseases (3–5). For example, both AD and PD have been associated with increased production of reactive oxygen species, which could result from genetic predisposition and/or environmental factors, such as exposure to pesticides (4). Post-mortem analyses reveal that the overall levels of oxidative damage to proteins, lipids, and DNA are elevated in AD and PD brains (6, 7). The most widely used marker for oxidative damage to proteins is the presence of carbonyl groups, which can be introduced into proteins by direct oxidation of Pro, Arg, Lys, and Thr side chains or by Michael addition reactions with products of lipid peroxidation or glycooxidation (3). Elevation in the total level of protein carbonyls has been documented in both AD and PD (6, 7). However, the identities of the oxidized proteins modified by carbonylation or other types of oxidation remain largely unknown. Furthermore, it remains to be determined whether the protein targets of oxidative damage are the same or different in AD and PD.

As a first step toward a molecular understanding of the pathogenic mechanism of oxidative stress in neurodegenerative diseases, we performed a search for specific protein targets of oxidative damage in AD and PD brains by using a proteomic approach that combined two-dimensional gel electrophoresis, immunological detection of protein oxidation, and mass spectrometry (8). Here we report that Cu,Zn-superoxide dismutase (SOD1; EC 1.15.1.1) is a major target of oxidative damage in AD and PD brains. SOD1 is a key antioxidant enzyme that catalyzes the disproportionation of superoxide radicals into molecular oxygen and hydrogen peroxide, which is then decomposed by catalase and glutathione peroxidase (9). Mutations in SOD1 have been identified as the cause for autosomal dominant familial form of ALS, a neurodegenerative disorder characterized by the loss of motor neurons in the spinal cord and brain (10–12). However, little is currently known about the role of SOD1 in the more common, sporadic form of ALS and in other neurodegenerative diseases, such as AD and PD. In the present study, we investigated the changes in the expression, localization, and oxidative modifications of SOD1 in the brains of patients with idiopathic AD or PD. Our results suggest that oxidative damage to and aggregation of SOD1 play a crucial role in the neurodegeneration associated with AD and PD.

MATERIALS AND METHODS

Human Brain Samples—Frontal cortex tissues from five clinically diagnosed PD patients, five AD patients, and five healthy non-demented control subjects (Table I) were obtained from the Emory Alzheimer Disease Center brain bank. The neuropathological diagnosis of PD was based

* This work was supported by National Institutes of Health Grants AG021489 and NS047575 (to L. L.), the Emory University Research Committee and Emory Collaborative Center Grant ES012068 for Environmental Research on Parkinson Disease (to L.-S. C.), and the Emory Center for Neurodegenerative Disease-Merck Scholar Award (to L. L.). The costs of publication of this article were defrayed in part by the payment of page charges. This article must therefore be hereby marked "*advertisement*" in accordance with 18 U.S.C. Section 1734 solely to indicate this fact.

‖ To whom correspondence should be addressed: Dept. of Pharmacology, Emory University School of Medicine, 1510 Clifton Rd., Atlanta, GA 30322-3090. Tel.: 404-727-5987; Fax: 404-727-0365; E-mail: lianli@pharm.emory.edu.

[1] The abbreviations used are: AD, Alzheimer disease; PD, Parkinson disease; ALS, amyotrophic lateral sclerosis; DNP, 2,4-dinitrophenyl; MALDI-TOF, matrix-assisted laser desorption ionization time-of-flight; ESI, electrospray ionization; MS/MS, tandem mass spectrometry; HPLC, high pressure liquid chromatography; SOD1, superoxide dismutase; Aβ, β-amyloid.

This paper is available on line at http://www.jbc.org

This is an Open Access article under the CC BY license.

TABLE I
Demographic data of human subjects

Subject	Age[a]	Sex		ApoE genotype[b]	PMI[c]
		Male	Female		
	yr				*h*
Control	76.0 ± 11.0	1	4	2/3 (2), 3/3 (3)	9.3 ± 6.8
PD	72.5 ± 6.5	5	0	2/3 (2), 3/3 (3)	5.2 ± 3.8
AD	70.5 ± 20.5	1	4	3/3 (2), 3/4 (2), 4/4 (1)	7.6 ± 4.8

[a] Values represent means ± S. D.
[b] The number of subjects of each genotype is given in parentheses.
[c] Post-mortem interval (PMI) values represent means ± S. D.

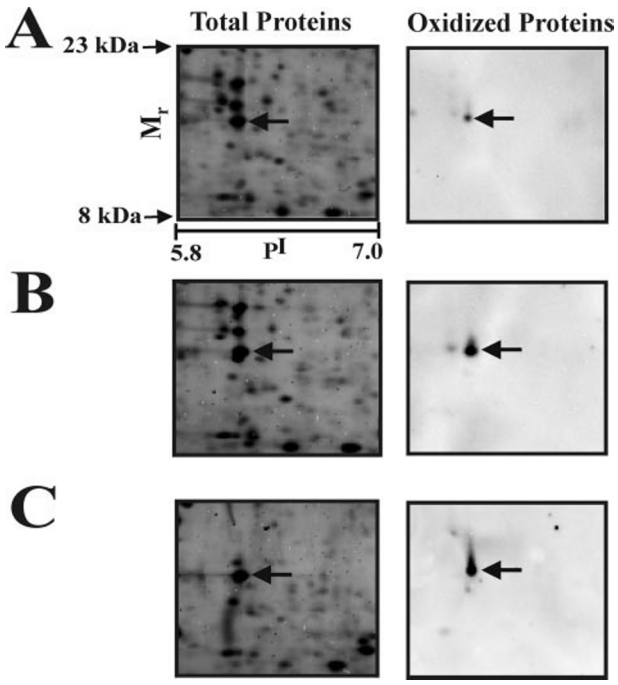

FIG. 1. **Oxidation of specific proteins in AD and PD brains.** Protein samples of control (*A*), PD (*B*), and AD (*C*) brains (350 μg) were subjected to two-dimensional gel electrophoresis, followed by SYPRO Ruby staining for total proteins (*left panels*) or by immunostaining with anti-DNP antibody for oxidized proteins (*right panels*). *Arrows* indicate a protein spot with apparent molecular mass/pI of 16 kDa/6.0 that exhibits elevated oxidation in both AD and PD.

on the presence of nigral degeneration and Lewy bodies. The diagnosis of AD was established using Consortium to Establish a Registry for Alzheimer Disease (CERAD) criteria (13). ApoE genotypes (Table I) were determined for all subjects as described previously (14).

Sample Preparation, DNP Derivatization, and Two-dimensional Gel Electrophoresis—Brain tissues were homogenized in a buffer containing 50 mM Tris-HCl and protease inhibitors (1 mM phenylmethylsulfonyl fluoride, 0.5 mg/ml benzamidine, 1 μM aprotinin, 10 μM leupeptin, 1 μM pepstatin A, and 1 μM bestatin), followed by centrifugation at 13,000 × *g*. Protein samples (350 μg) were applied to 17-cm immobilized pH gradient strips (pH 4–7) in an immobilized pH gradient re-swelling tray, and the strips were then isoelectrically focused on a Protein IEF Cell (Bio-Rad) for 24,000 V-h (15). Following isoelectric focusing, the strips were immediately subjected to in-strip DNP derivatization as described previously (16) by a 15-min incubation in 2 N HCl/10 mM 2,4-dinitrophenylhydrazine at 25 °C. After being washed with 2 M Tris base/30% (v/v) glycerol for 15 min, the strips were equilibrated for 15 min in 50 mM Tris-HCl (pH 8.8) containing 6 M urea, 2% (w/v) SDS, 30% (v/v) glycerol, and 1.0% (w/v) dithiothreitol. The strips were then re-equilibrated for 15 min in the same buffer containing 2.5% (w/v) iodoacetamide instead of dithiothreitol. Second-dimension separation was performed on SDS-polyacrylamide gradient gels (10–20% porosity polyacrylamide) using the Ettan-DALT slab gel SDS-PAGE system (Amersham Biosciences).

SYPRO Ruby Staining—Duplicate samples of brain proteins were subjected to two-dimensional gel electrophoresis as described above. Proteins in one gel were stained with SYPRO Ruby protein gel stain (Bio-Rad), whereas proteins in the other gel were electroblotted to polyvinylidene difluoride membranes using the Ettan-DALT system. For SYPRO Ruby staining, proteins were first fixed in the gel using 40% methanol/10% acetic acid (v/v) for 30 min. The gel was then incubated in SYPRO Ruby protein gel stain solution overnight and subsequently destained using 10% methanol/6% acetic acid (v/v) for 45 min. The SYPRO Ruby-stained gel was placed in a light-tight cabinet directly on a transilluminator, and the fluorescence generated by excitation with UV light at 365 nm was recorded using a cooled, computerized charge-coupled device camera-based imaging system (Alpha Innotech, San Leandro, CA).

TABLE II
Increased oxidation of the 16-kDa/pI 6.0 protein spot in PD and AD brains compared to controls

The specific oxidation index of the spot in Fig. 1 was obtained by normalization of the intensity of the anti-DNP immunostain to the intensity of the protein stain. Values represent means ± S. E. for five individuals of each of the PD, AD, or control group.

Samples (n = 5)	Specific oxidation index
Control	4.9 ± 0.9
PD	44.2 ± 8.9[a]
AD	36.5 ± 6.0[a]

[a] $p < 0.05$.

Immunoblotting and Image Analyses—The polyvinylidene difluoride membranes were removed from the Ettan-DALT electroblotting apparatus and incubated for 1 h with phosphate-buffered saline containing 3% (v/v) Tween and 5% (w/v) nonfat dried skim milk (PBS-TM). Membranes were incubated overnight at 4 °C with anti-DNP primary antibody (Molecular Probes, Eugene, OR) at a 1:16,000 dilution or with anti-SOD1 antibody (Santa Cruz Biotechnology, Inc., Santa Cruz, CA) at a 1:2000 dilution as described previously (17). After extensive washing with PBS-TM, the membranes were incubated for 1 h at 4 °C with a 1:16,000 dilution of horseradish peroxidase-conjugated goat anti-rabbit secondary antibody (Sigma). Immunostained proteins were detected by using a SuperSignal chemiluminescence kit (Pierce) and an Alpha Innotech imaging system. Digitized images from SYPRO Ruby-stained gels and immunoblots were analyzed using the two-dimensional electrophoresis gel analysis program PD Quest (Bio-Rad). The data were analyzed statistically by analysis of variance.

Mass Spectrometry—Spots of interest were excised from the gels and digested *in situ* with trypsin (modified; Promega, Madison, WI). The resulting digests were subjected to matrix-assisted laser desorption ionization time-of-flight (MALDI-TOF) mass spectrometry and capillary HPLC-electrospray ionization (ESI) tandem mass spectrometry (MS/MS). MALDI-TOF mass spectra were acquired on an Applied Biosystems Voyager-DE STR. The peptide mass maps produced by MALDI-TOF mass spectrometry were searched against the published databases by means of Mascot (Matrix Science) and the MS Fit component of Protein Prospector (prospector.ucsf.edu/ucsfhtml4.0/msfit.htm). Electrospray ionization mass spectra were acquired on a Finnigan LCQ ion trap mass spectrometer adapted for microspray ionization sample introduction. On-line HPLC separation of the tryptic peptides was accomplished with a Michrom MAGIC 2002 micro HPLC: column, PicoFrit™ (New Objective; 75-μm inner diameter) packed to 10 cm with C18 adsorbent (Vydac; 218MSB5; 5 μm, 300 Å); mobile phase A, 0.5% acetic acid/0.005% trifluoroacetic acid; mobile phase B, 90% acetonitrile/0.5% acetic acid/0.005% trifluoroacetic acid; linear gradient of 2–72% B in 30 min; flow rate, 0.4 μl/min. As a part of the data-dependent acquisition protocol, the four most intense ions in each survey scan were sequentially fragmented in the ion trap by collision-induced dissociation using an isolation width of 2.5 and a relative collision energy

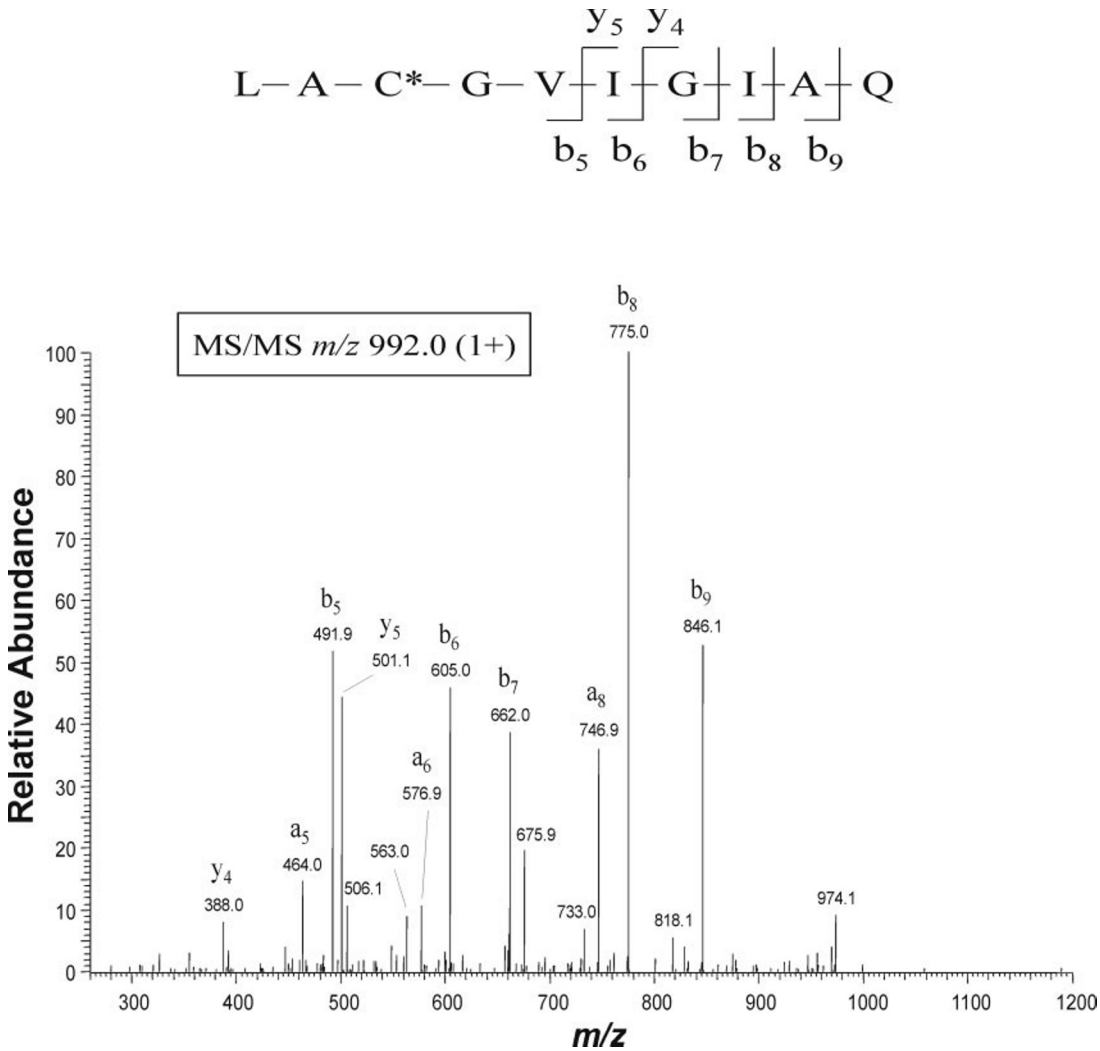

FIG. 2. **Identification of the oxidized protein spot in Fig. 1 as SOD1 by mass spectrometry.** The protein spot indicated in Fig. 1 was excised from the two-dimensional gels and analyzed by HPLC-ESI tandem mass spectrometry. Collision-induced dissociation mass spectrum of the ion at m/z 992.0 (1+) in AD and PD brains indicates the identity of this ion as SOD1 peptide 144–153. Peptide fragments are indicated using the nomenclature of Roepstorff and Fohlman (41). *C**, cysteic acid.

of 35%. Uninterpreted MS/MS spectra were analyzed by the SEQUEST component of the LCQ software and by Mascot (Matrix Science). Assignment of the MS/MS fragments was verified by comparison with the predicted ions generated *in silico* by GPMAW (Lighthouse Data).

Immunohistochemistry—Brains were fixed in 4% paraformaldehyde and cryoprotected in sucrose, and serial sections (50 μm) of cingulate cortex were cut on a cryostat. Sections were treated with 3% H_2O_2 to eliminate endogenous peroxidase activity and blocked with a solution containing 8% goat serum, 10 μg/ml avidin, 0.1% Triton X-100, 0.9% NaCl, and 50 mM Tris-HCl (pH 7.2). Sections were then incubated overnight at 4 °C with mouse monoclonal anti-SOD1 antibody (0.5 μg/ml; BD Biosciences) or monoclonal anti-Aβ antibody (4G8; 1:5000; Signet) followed by incubation with biotinylated secondary antibody (1:200). Bound antibodies were detected using a standard avidin-biotinylated peroxidase complex method (Vectastain Elite ABC kit; Vector Laboratories). Sections were observed using a Leica DC500 microscope, and images were captured with a C4742-95 Hamamatsu digital camera.

Double Fluorescence Labeling Confocal Microscopy—Brain tissues from patients with Alzheimer disease were fixed in 4% paraformaldehyde for 2–3 days. Blocks of cingulate cortex were cryoprotected in 30% sucrose, and frozen sections were cut on a sliding microtome at 50 μm. Sections were rinsed in phosphate-buffered saline, treated with 3% H_2O_2, and blocked with normal horse serum (8%), avidin (10 μg/ml), and Triton X-100 (0.1%) in Tris-buffered saline for 1 h before incubation with mouse monoclonal antibody to SOD1 (1 μg/ml; BD Biosciences) in Tris-buffered saline containing 50 μg/ml biotin for 2 days at 4 °C. Following Tris-buffered saline rinses, sections were incubated with biotinylated goat anti-mouse secondary antibody (1:200; Vector Laboratories), followed by detection using the avidin-biotinylated peroxidase complex method. Signal amplification was achieved using tyramide-Cy3 reagent (PerkinElmer Life Sciences). Sections were counterstained with 1% thioflavin S (Sigma-Aldrich) for 20 min, rinsed in 70% ethanol, and coverslipped. Images were acquired using a Zeiss LSM510 Meta confocal microscope.

RESULTS

Molecular Characterization of Altered Protein Oxidative Modification in AD and PD Brains—To investigate alterations in protein oxidation associated with AD and PD, we performed comparative high-resolution, two-dimensional gel electrophoresis experiments on protein samples obtained from AD and PD brains and age-matched controls (Table I). Brain protein extracts were resolved by isoelectric focusing on an immobilized pH gradient strip followed by in-strip DNP derivatization (reacting with protein carbonyls) and second-dimensional separation by SDS-PAGE. Total proteins in the two-dimensional gels were visualized by staining with SYPRO Ruby, and oxidatively modified proteins were detected by immunoblotting with anti-DNP antibody. Comparison of anti-DNP immunoblots with SYPRO Ruby-stained two-dimensional gels revealed that a protein spot that electrophoresed on the two-dimensional gel with apparent molecular mass/pI values of 16 kDa/6.0 exhibited enhanced oxidation in AD and PD brains (Fig. 1).

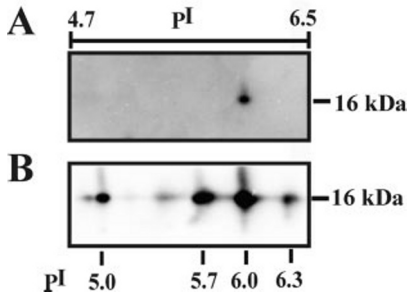

FIG. 3. **Identification of four SOD1 isoforms and confirmation of the identified oxidized protein as the SOD1 pI 6.0 isoform.** Protein extracts (350 μg) from a PD brain were subjected to two-dimensional gel electrophoresis, followed by immunoblotting with anti-DNP antibody (*A*) or anti-SOD1 antibody (*B*). The result shows four SOD1 isoforms with different pI values. The oxidized protein spot identified by mass spectrometry as SOD1 represents the pI 6.0 isoform of SOD1.

Quantification results showed that the specific oxidation level of this spot was increased ~7.5-fold in AD and 9-fold in PD compared with age-matched control brains (Table II).

Identification of SOD1 as a Major Target of Oxidative Damage in AD and PD Brains by Mass Spectrometry—For determination of the identity of the oxidized protein spot indicated in Fig. 1, the spot was excised from the two-dimensional gels, and its identity was determined by mass spectrometric analysis. The spot was unambiguously identified as human Cu,Zn-superoxide dismutase (SOD1; GenBank™ accession number NP_000445; Swiss-Prot accession number P00441) by using HPLC-electrospray ionization tandem mass spectrometry (Fig. 2). This assignment is further strengthened by the agreement between the apparent molecular mass/pI values (16 kDa/6.0) of the protein spot and the predicted values of 15.9 kDa/5.7 for human SOD1. Mass spectrometric data indicated that Cys-146, a cysteine residue in the C-terminal region of SOD1, was oxidized to cysteic acid (also known as cysteine sulfonic acid, Cys-SO_3H) in AD and PD brains (Fig. 2).

Immunoblot Analysis Reveals the Presence of Four Brain SOD1 Isoforms and Confirms the Identified Oxidized Protein as the SOD1 pI 6.0 Isoform—To confirm the protein identification result obtained by mass spectrometry, we performed two-dimensional gel electrophoresis of human brain samples followed by immunoblotting with a rabbit polyclonal anti-SOD1 antibody. As shown in Fig. 3, anti-SOD1 antibody specifically recognized four distinct protein spots with the same molecular mass (16 kDa) and different isoelectric points (pI = 6.3, 6.0, 5.7, and 5.0, respectively), demonstrating the presence of four SOD1 isoforms in human brain. Of these four SOD1 spots, only one spot (pI = 6.0) was immunoreactive to anti-DNP antibody, indicating that the pI 6.0 isoform of SOD1 was oxidatively modified by carbonyl formation (Fig. 3, *A* and *B*). The specific oxidation of the 16-kDa/pI 6.0 SOD1 spot is consistent with the results described in Fig. 1.

The SOD1 pI 5.0 Isoform Is Selectively Accumulated in AD and PD Brains—We next examined whether or not the four SOD1 isoforms were differentially expressed in AD, PD, and control brains by two-dimensional immunoblot analysis (Fig. 4, *A*–*C*). Quantification results (Fig. 4*D*) showed a more than 6-fold increase in the relative level of the pI 5.0 isoform of SOD1 in AD and PD brains compared with age-matched controls. The different isoelectric points of the SOD1 isoforms (Fig. 4) suggest the presence of some types of post-translational modification that alter the charge of SOD1 protein. To test this possibility, the four different pI spots of SOD1 were individually excised from the two-dimensional gels, and their tryptic digests were analyzed by MALDI-TOF/MS/MS and HPLC-ESI/MS/MS. Despite repeated attempts, efforts to identify the post-translational modification that causes the pI shifts of SOD1 have so far been unsuccessful.

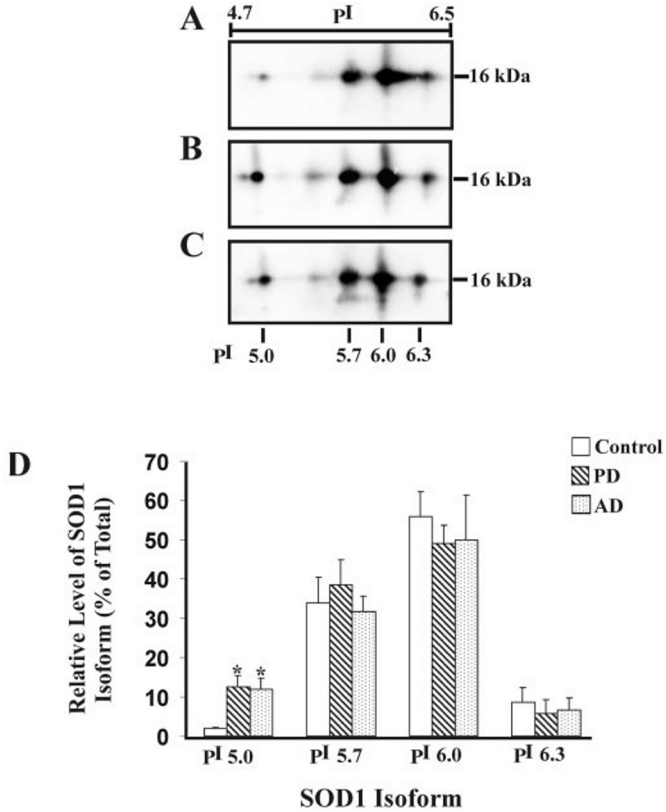

FIG. 4. **Accumulation of SOD1 pI 5.0 isoform in AD and PD brains.** Protein samples of control (*A*), PD (*B*), and AD (*C*) brains were subjected to two-dimensional gel electrophoresis, followed by immunoblotting with anti-SOD1 antibody. *D*, the relative level of each SOD1 isoform was measured by quantification of the intensity of the individual SOD1 isoform using the two-dimensional gel analysis program PD Quest and expressed as a percentage of the total level of all four SOD1 isoforms. Values represent the means ± S.E. for five PD, five AD, and five control individuals. The *asterisk* indicates a statistically significant ($p < 0.05$) increase in the level of the SOD1 pI 5.0 isoform in PD or AD *versus* control.

The Total Level of SOD1 Protein Is Increased in AD and PD Brains—Our two-dimensional immunoblotting data (Fig. 4) suggest that the total level of all four SOD1 isoforms is increased in AD and PD brains. To further investigate this possibility, we performed quantitative Western blot analysis using protein samples obtained from AD and PD brains and age-matched controls (Table I). The fact that all four SOD1 isoforms have the same molecular mass (Fig. 3) allowed us to use one-dimensional gel electrophoresis for direct comparison of the total SOD1 levels of various brain samples on the same gel. After electrophoresis, the gels were subjected to immunoblotting with antibodies against SOD1 and actin. The relative level of SOD1 in each sample was measured by quantification of the intensity of the SOD1 band and normalized to the actin level in the corresponding sample (Fig. 5). The results indicated that the total level of SOD1 was increased 2.4-fold in PD brains and 2.5-fold in AD brains compared with controls.

Accumulation of SOD1 Protein Aggregates in AD Brains—Oxidative modification may convert proteins into forms that are more prone to aggregation and/or more resistant to proteolytic degradation, resulting in the formation of protein aggregates (18). Because our biochemical data revealed that SOD1 was significantly oxidized and accumulated in AD and PD brains, we used immunohistochemistry to investigate whether

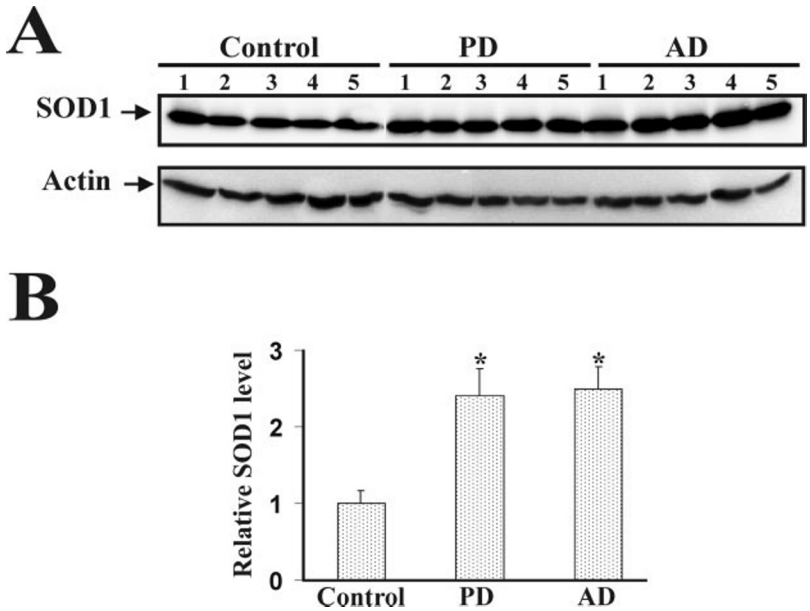

FIG. 5. **The total level of SOD1 protein is increased in AD and PD brains.** *A*, protein extracts of control, PD, and AD brains were subjected to one-dimensional gel electrophoresis, followed by immunoblotting with anti-SOD1 antibody. Each *lane* represents a different individual from the control, PD, and AD groups. *B*, the relative SOD1 level was measured by quantification of the intensity of the 16-kDa SOD1 band and normalized to the actin level in the corresponding brain extract. The *bar graph* shows the results (means ± S.E.) from five PD, five AD, and five control individuals. The *asterisk* indicates a statistically significant ($p < 0.05$) increase in the total level of SOD1 protein in PD or AD *versus* control.

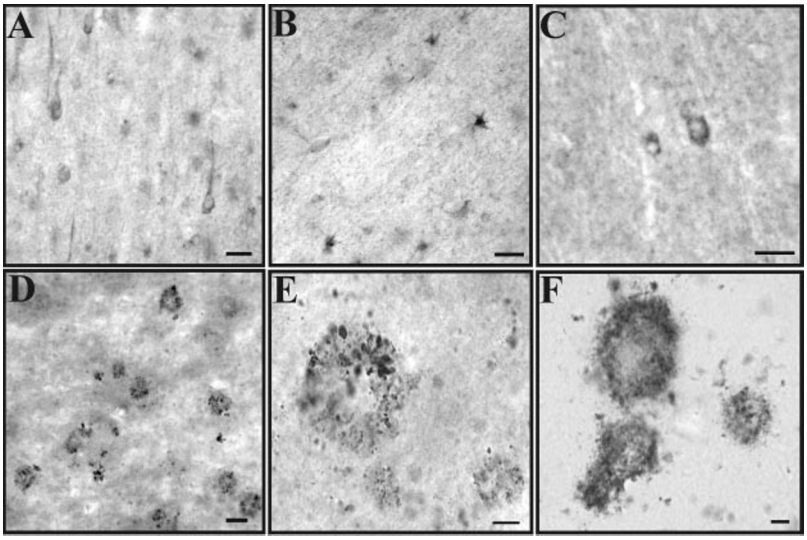

FIG. 6. **Immunohistochemical analysis of SOD1 expression in PD, AD, and control brains.** Sections of cingulate cortical regions from control (*A* and *B*), PD (*C*), or AD (*D*–*F*) brains were immunostained with antibodies against SOD1 (*A*–*E*) or Aβ (*F*). *Scale bar* = 20 μm in *A*, *B*, and *D*; 10 μm in *C*, *E*, and *F*.

SOD1 aggregates in these diseases. In control human brains, intense SOD1 immunoreactivity was observed in pyramidal neurons in addition to moderately stained neurons and neuropils throughout the neocortex (Fig. 6*A*). Strong SOD1 immunostaining was also found in astrocytes in white matter (Fig. 6*B*). PD brains exhibited similar SOD1 immunostaining patterns compared with the controls (data not shown). However, aggregation of SOD1 protein was occasionally seen in the cytoplasm of some neurons (Fig. 6*C*), although we did not detect SOD1 immunoreactivity in Lewy bodies of PD brains (data not shown). In AD brains, prominent SOD1 immunoreactivity was observed in aggregates with granular or globular appearances (Fig. 6, *D* and *E*). Many of these SOD1-positive deposits had diameters similar to amyloid plaques labeled by anti-Aβ antibody in adjacent brain sections (Fig. 6*F*).

SOD1 Aggregates Are Associated with Senile Plaques and Neurofibrillary Tangles in AD Brains—To further characterize SOD1 aggregates, we performed double fluorescence labeling experiments using anti-SOD1 antibody and thioflavin S, a widely used dye that binds to fibrillar, β-pleated sheet structures. As shown in Figs. 7 and 8, there was very little overlap between SOD1 immunostaining and thioflavin S labeling, suggesting that SOD1 aggregates *per se* are amorphous protein deposits with little fibrillar, β-pleated sheet content. However, SOD1 aggregates were closely associated with thioflavin S-positive amyloid plaques (Fig. 7) and neurofibrillary tangles and neuropil threads (Fig. 8).

DISCUSSION

SOD1 is a ubiquitously expressed antioxidant enzyme that plays a key role in the cellular defense against harmful superoxide radicals (9, 19). The importance of SOD1 in neurodegeneration was first discovered by the identification of more than 100 different point mutations in SOD1 as causative genetic defects for familial ALS (20). In this study, we found that SOD1 is one of the major targets of oxidative damage in AD and PD brains and provided evidence supporting the involvement of oxidative damage to and aggregation of SOD1 in the two common neurodegenerative disorders AD and PD.

By using a combination of two-dimensional gel electrophoresis, immunoblot analysis, and mass spectrometry, we have identified four human brain SOD1 isoforms with pI values of 6.3, 6.0, 5.7, and 5.0, respectively. The chemical nature of the modifications responsible for the differences in the pI value of the SOD1 isoforms remains to be determined. It is possible that some of the SOD1 pI isoforms represent differentially metallated forms of SOD1. SOD1 is a homodimeric metalloprotein containing one Cu(II) and one Zn(II) ion per subunit (19). SOD1

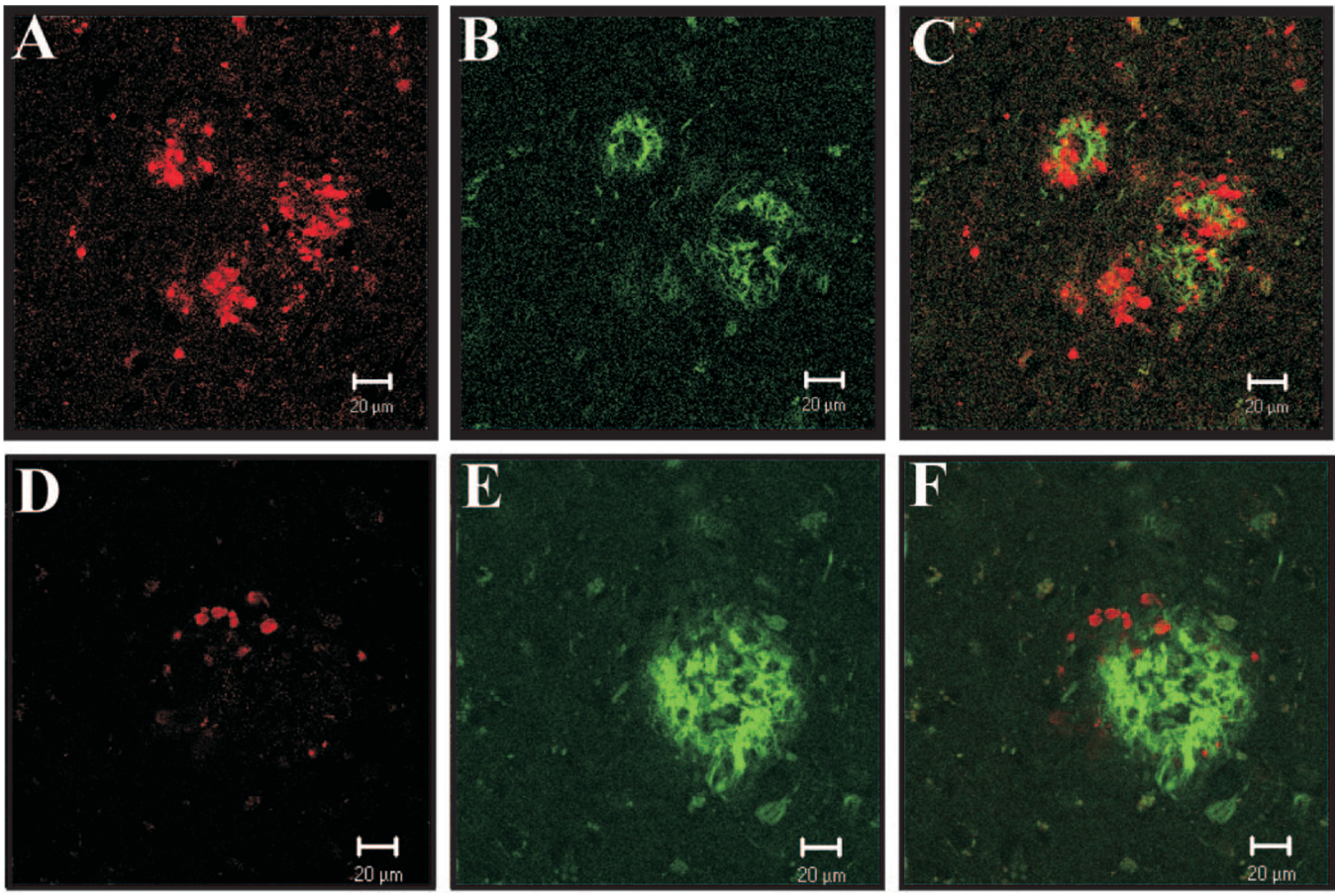

FIG. 7. **Association of SOD1 aggregates with senile plaques in AD brains.** Sections of cingulate cortical regions from AD brains were stained with anti-SOD1 antibody (*A* and *D*) and thioflavin S (*B* and *E*). Images were obtained by confocal microscopy. Superimposed images (*C* and *F*) revealed the association of SOD1 aggregates with thioflavin S-positive amyloid plaques.

protein is known to first fold into a dimeric apo form and then acquires Cu(II) from the copper chaperone for SOD1 (21). Although the mechanism of the Zn(II) acquisition is not yet known, Zn-deficient wild-type and mutant SOD1 have been implicated in ALS (19, 22). The predicted pI of SOD1 in its metallated holo form, partially metallated form (Cu-free or Zn-free state), and metal-free apo form is 6.4, 6.0, and 5.7, respectively. We observed that in the control human brains, SOD1 exists mainly in three isoforms (pI = 6.3, 6.0, and 5.7), of which the pI 6.0 and pI 5.7 isoforms are most abundant, accounting for about 55% and 35% of total SOD1 protein, respectively. The observed pI 6.0 isoform is likely to be the metallated holo form of SOD1, whereas the pI 5.7 isoform may represent the partially metallated form. Consistent with this assumption, copper incorporation experiments revealed that the Cu-free form of SOD1 constitutes ~35% of the total SOD1 in human lymphoblasts (23).

Our data showed no significant change in the relative levels of pI 6.3, pI 6.0, and pI 5.7 isoforms of SOD1 in AD and PD brains compared with age-matched controls. In contrast, the level of the more acidic SOD1 isoform (pI = 5.0) is increased more than 6-fold in AD and PD brains. The selective accumulation of the acidic SOD1 pI isoform is analogous to the acidic pI shift of familial PD-associated DJ-1 protein in response to oxidative stress (24, 25). In the case of DJ-1, the acid pI shift is thought to result from direct oxidation of DJ-1 by H_2O_2, leading to the formation of cysteine sulfinic or sulfonic acid (24, 25). A similar oxidative modification of SOD1 might be responsible for accumulation of the acidic SOD1 pI 5.0 isoform in AD and PD brains.

Our proteomic results indicated that the SOD1 pI 6.0 isoform, but not the other three SOD1 isoforms (pI = 6.3, 5.7, and 5.0), is heavily oxidized in AD and PD brains by carbonylation, an irreversible oxidative modification that is widely used as a marker of oxidative damage (3). A 7.5–9-fold increase in the specific oxidation level of the SOD1 pI 6.0 isoform was observed in AD and PD brains compared with age-matched control brains, providing the first direct evidence for occurrence of oxidative damage to SOD1 in sporadic AD and PD. In addition, we found that Cys-146 of the SOD1 pI 6.0 isoform is oxidized irreversibly to cysteine sulfonic acid in AD and PD brains. Cysteine contains a thiol group (Cys-SH) that can be reversibly oxidized to a sulfenic acid (Cys-SOH) or sulfinic acid (Cys-SO_2H) by low concentrations of H_2O_2 and irreversibly oxidized to a sulfonic acid (Cys-SO_3H) by high concentrations of H_2O_2 (26–28). The identified irreversible cysteine oxidation of SOD1 is consistent with previous *in vitro* studies showing that SOD1 undergoes oxidative damage by its own reaction product H_2O_2 (29, 30). The vulnerability of SOD1 to H_2O_2-mediated oxidative damage underscores the importance of H_2O_2 clearance by catalase and peroxidases. Elevated levels of H_2O_2 in the brain have been implicated in AD and PD (6). It has been shown that Aβ peptide can directly catalyze the production of H_2O_2 *in vitro*, suggesting that Aβ deposits may be a source of H_2O_2 in AD brain (31, 32). The increased H_2O_2 levels in AD and PD may overwhelm the cellular H_2O_2 defense systems, leading to various oxidative products, including oxidized SOD1.

Our findings raise a possibility that the identified oxidative modifications of SOD1 might contribute to the pathogenesis of

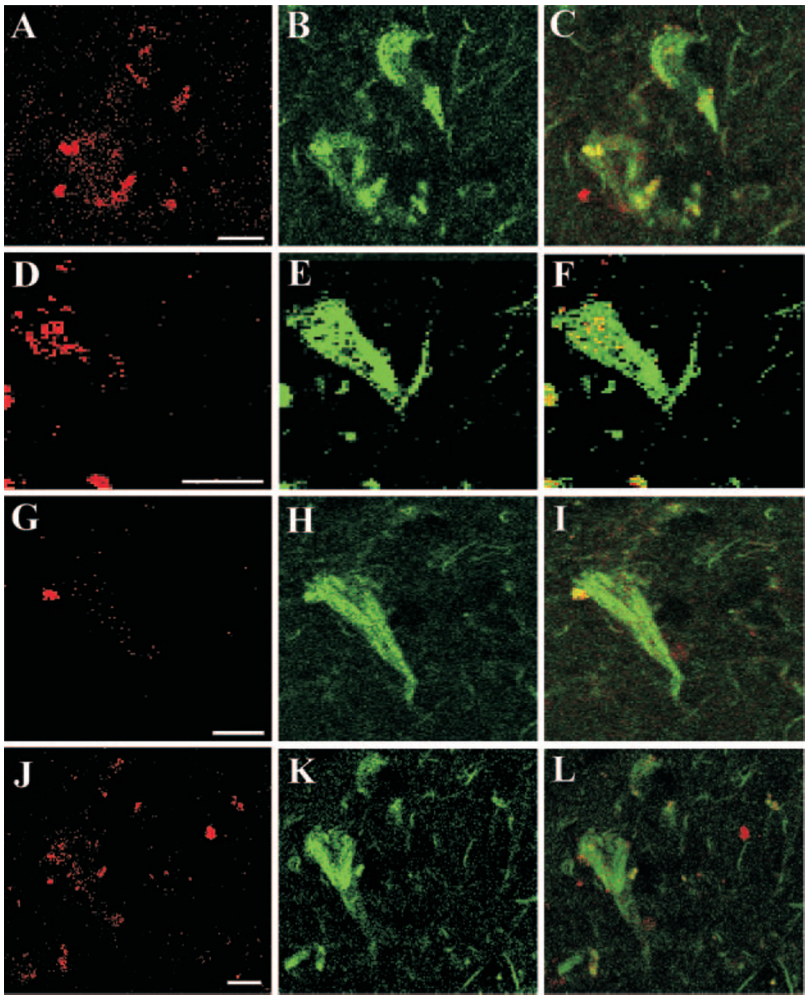

FIG. 8. **Association of SOD1 aggregates with neurofibrillary tangles in AD brains.** Sections of cingulate cortical regions from AD brains were stained with anti-SOD1 antibody (*A*, *D*, *G*, and *J*) and thioflavin S (*B*, *E*, *H*, and *K*). Images were obtained by confocal microscopy. Superimposed images (*C*, *F*, *I*, and *L*) revealed the association of SOD1 aggregates with thioflavin S-positive neurofibrillary tangles. *Scale bar* = 10 μm.

sporadic AD and PD in a manner similar to the genetic mutations of SOD1 in causing neurodegeneration in familial ALS. In agreement with this possibility, Cys-146, a cysteine residue that we found to be irreversibly oxidized in AD and PD brains, is mutated to an arginine (C146R) in familial ALS (33). Ample evidence indicates that SOD1 mutations cause neurodegeneration by a gain of cytotoxic function, rather than a loss of enzymatic activity (19, 20). Transgenic mice expressing familial ALS-associated mutant SOD1 develop severe motor neuron degeneration (34), whereas neither transgenic mice expressing the human wild-type SOD1 (35) nor SOD1 knock-out mice (36) exhibit such an ALS-like phenotype. The mechanism by which SOD1 mutants cause neurodegeneration is not understood, but it has been suggested that the toxic gain of function is a consequence of mutation-induced misfolding of SOD1, which leads to the formation of cytotoxic SOD1 aggregates (11, 19). The oxidative modifications of SOD1 identified in AD and PD brains may induce misfolding and/or protease resistance of SOD1, thereby promoting the accumulation and aggregation of SOD1. In support of this possibility, we found that the total level of SOD1 protein is significantly increased in both AD and PD. Moreover, we observed the presence of prominent SOD1-immunoreactive protein aggregates in AD brains. These aggregates are unlikely to be nonspecific staining artifacts of the anti-SOD1 antibody because similar SOD1 aggregates have been observed in AD brains using different anti-SOD1 antibodies (37). Although we were unable to detect SOD1 immunostaining in Lewy bodies in our PD samples, the previously reported association of SOD1 with Lewy bodies (38) is consistent with our hypothesis.

We have further characterized SOD1 aggregates in AD brains by double fluorescence labeling confocal microscopy and found that these aggregates are not stained with thioflavin S, indicating that SOD1 aggregates are not fibrillar amyloid deposits. The granular morphology and non-fibrillar nature of SOD1 aggregates in AD brains resemble the SOD1-positive inclusion bodies found in both familial and sporadic forms of ALS (12, 39, 40). In AD brains, we found that SOD1 aggregates are closely associated with amyloid senile plaques and neurofibrillary tangles. The co-occurrence of SOD1 aggregates with the hallmark lesions of AD and PD suggests a common or overlapping mechanism(s) underlying the formation of pathological inclusions in AD, PD, and ALS.

Although the genetic defects underlying some of the rare familial forms of AD, PD, and ALS have recently been identified, the causes of the common, sporadic forms of these diseases remain unclear. Our work suggests that oxidative damage to and subsequent aggregation of SOD1 may contribute to the neurodegeneration associated with AD and PD. It would be worthwhile to determine whether the identified oxidative modifications of SOD1 also take place in sporadic ALS. The overlapping pathogenic mechanisms of these neurodegenerative diseases raise an exciting possibility that similar potential therapeutic strategies might be utilized for treating these disorders.

Acknowledgment—We thank Christopher A. Carroll of the Institutional Mass Spectrometry Laboratory at the University of Texas Health Science Center at San Antonio (supported in part by National Institutes of Health Grant CA54174) for mass spectrometric analyses.

REFERENCES

1. Ciechanover, A., and Brundin, P. (2003) *Neuron* **40,** 427–446
2. Bossy-Wetzel, E., Schwarzenbacher, R., and Lipton, S. A. (2004) *Nat. Med.* **10,** (suppl.) S2–S9
3. Levine, R. L., and Stadtman, E. R. (2001) *Exp. Gerontol.* **36,** 1495–1502
4. Beal, M. F. (2002) *Free Radic. Biol. Med.* **32,** 797–803
5. Ischiropoulos, H., and Beckman, J. S. (2003) *J. Clin. Investig.* **111,** 163–169
6. Giasson, B. I., Ischiropoulos, H., Lee, V. M., and Trojanowski, J. Q. (2002) *Free Radic. Biol. Med.* **32,** 1264–1275
7. Jenner, P. (2003) *Ann. Neurol.* **53,** Suppl. 3, S26–S36; discussion S36–S38
8. Choi, J., Levey, A. I., Weintraub, S. T., Rees, H. D., Gearing, M., Chin, L. S., and Li, L. (2004) *J. Biol. Chem.* **279,** 13256–13264
9. Fridovich, I. (1995) *Annu. Rev. Biochem.* **64,** 97–112
10. Rosen, D. R., Siddique, T., Patterson, D., Figlewicz, D. A., Sapp, P., Hentati, A., Donaldson, D., Goto, J., O'Regan, J. P., Deng, H. X., Rahmani, Z., Krizus, A., McKenna-Yasek, D., Cayabyab, A., Gaston, S., Tanzi, R., Halperin, J. J., Herzfeldt, B., Van den Berg, R., Hung, W., Bird, T., Deng, G., Mulder, D. W., Smith, C., Laing, N. G., Soriano, E., Pericak-Vance, M. A., Haines, J., Rouleau, G. A., Gusella, J., Horvitz, H. R., and Brown, R. H., Jr. (1993) *Nature* **362,** 59–62
11. Cleveland, D. W., and Rothstein, J. D. (2001) *Nat. Rev. Neurosci.* **2,** 806–819
12. Bruijn, L. I., Miller, T. M., and Cleveland, D. W. (2004) *Annu. Rev. Neurosci.* **27,** 723–749
13. Mirra, S. S., Heyman, A., McKeel, D., Sumi, S. M., Crain, B. J., Brownlee, L. M., Vogel, F. S., Hughes, J. P., van Belle, G., and Berg, L. (1991) *Neurology* **41,** 479–486
14. Gearing, M., Schneider, J. A., Rebeck, G. W., Hyman, B. T., and Mirra, S. S. (1995) *Neurology* **45,** 1985–1990
15. Choi, J., Malakowsky, C. A., Talent, J. M., Conrad, C. C., and Gracy, R. W. (2002) *Biochem. Biophys. Res. Commun.* **293,** 1566–1570
16. Conrad, C. C., Choi, J., Malakowsky, C. A., Talent, J. M., Dai, R., Marshall, P., and Gracy, R. W. (2001) *Proteomics* **1,** 829–834
17. Choi, J., Conrad, C. C., Malakowsky, C. A., Talent, J. M., Yuan, C. S., and Gracy, R. W. (2002) *Biochim. Biophys. Acta* **1571,** 201–210
18. Stadtman, E. R. (2001) *Ann. N. Y. Acad. Sci.* **928,** 22–38
19. Valentine, J. S., and Hart, P. J. (2003) *Proc. Natl. Acad. Sci. U. S. A.* **100,** 3617–3622
20. Guegan, C., and Przedborski, S. (2003) *J. Clin. Investig.* **111,** 153–161
21. Rae, T. D., Schmidt, P. J., Pufahl, R. A., Culotta, V. C., and O'Halloran, T. V. (1999) *Science* **284,** 805–808
22. Julien, J. P. (2001) *Cell* **104,** 581–591
23. Petrovic, N., Comi, A., and Ettinger, M. J. (1996) *J. Biol. Chem.* **271,** 28331–28334
24. Mitsumoto, A., Nakagawa, Y., Takeuchi, A., Okawa, K., Iwamatsu, A., and Takanezawa, Y. (2001) *Free Radic. Res.* **35,** 301–310
25. Canet-Aviles, R. M., Wilson, M. A., Miller, D. W., Ahmad, R., McLendon, C., Bandyopadhyay, S., Baptista, M. J., Ringe, D., Petsko, G. A., and Cookson, M. R. (2004) *Proc. Natl. Acad. Sci. U. S. A.* **101,** 9103–9108
26. Claiborne, A., Yeh, J. I., Mallett, T. C., Luba, J., Crane, E. J., III, Charrier, V., and Parsonage, D. (1999) *Biochemistry* **38,** 15407–15416
27. Woo, H. A., Chae, H. Z., Hwang, S. C., Yang, K. S., Kang, S. W., Kim, K., and Rhee, S. G. (2003) *Science* **300,** 653–656
28. Forman, H. J., Fukuto, J. M., and Torres, M. (2004) *Am. J. Physiol. Cell Physiol.* **287,** C246–C256
29. Uchida, K., and Kawakishi, S. (1994) *J. Biol. Chem.* **269,** 2405–2410
30. Kurahashi, T., Miyazaki, A., Suwan, S., and Isobe, M. (2001) *J. Am. Chem. Soc.* **123,** 9268–9278
31. Huang, X., Atwood, C. S., Hartshorn, M. A., Multhaup, G., Goldstein, L. E., Scarpa, R. C., Cuajungco, M. P., Gray, D. N., Lim, J., Moir, R. D., Tanzi, R. E., and Bush, A. I. (1999) *Biochemistry* **38,** 7609–7616
32. Opazo, C., Huang, X., Cherny, R. A., Moir, R. D., Roher, A. E., White, A. R., Cappai, R., Masters, C. L., Tanzi, R. E., Inestrosa, N. C., and Bush, A. I. (2002) *J. Biol. Chem.* **277,** 40302–40308
33. de Belleroche, J., Orrell, R., and King, A. (1995) *J. Med. Genet.* **32,** 841–847
34. Gurney, M. E., Pu, H., Chiu, A. Y., Dal Canto, M. C., Polchow, C. Y., Alexander, D. D., Caliendo, J., Hentati, A., Kwon, Y. W., Deng, H. X., Chen, W., Zhai, P., Sufit, R. L., and Siddique, T. (1994) *Science* **264,** 1772–1775
35. Jaarsma, D., Haasdijk, E. D., Grashorn, J. A., Hawkins, R., van Duijn, W., Verspaget, H. W., London, J., and Holstege, J. C. (2000) *Neurobiol. Dis.* **7,** 623–643
36. Reaume, A. G., Elliott, J. L., Hoffman, E. K., Kowall, N. W., Ferrante, R. J., Siwek, D. F., Wilcox, H. M., Flood, D. G., Beal, M. F., Brown, R. H., Jr., Scott, R. W., and Snider, W. D. (1996) *Nat. Genet.* **13,** 43–47
37. Furuta, A., Price, D. L., Pardo, C. A., Troncoso, J. C., Xu, Z. S., Taniguchi, N., and Martin, L. J. (1995) *Am. J. Pathol.* **146,** 357–367
38. Nishiyama, K., Murayama, S., Shimizu, J., Ohya, Y., Kwak, S., Asayama, K., and Kanazawa, I. (1995) *Acta Neuropathol.* **89,** 471–474
39. Okamoto, K., Hirai, S., Yamazaki, T., Sun, X. Y., and Nakazato, Y. (1991) *Neurosci. Lett.* **129,** 233–236
40. Kato, S., Takikawa, M., Nakashima, K., Hirano, A., Cleveland, D. W., Kusaka, H., Shibata, N., Kato, M., Nakano, I., and Ohama, E. (2000) *Amyotroph Lateral Scler. Other Motor Neuron Disord.* **1,** 163–184
41. Roepstorff, P., and Fohlman, J. (1984) *Biomed. Mass Spectrom.* **11,** 601